Opto-Electronic Advances

Supplementary information

2018, Vol. 1, No. 6

DOI: 10.29026/oea.2018.180010

Mode evolution and nanofocusing of grating-coupled surface plasmon polaritons on metallic tip

Fanfan Lu[1], Wending Zhang[1]*, Ligang Huang[2], Shuhai Liang[1], Dong Mao[1], Feng Gao[3], Ting Mei[1]* and Jianlin Zhao[1]

[1]MOE Key Laboratory of Material Physics and Chemistry under Extraordinary Conditions and Shaanxi Key Laboratory of Optical Information Technology, School of Science, Northwestern Polytechnical University, Xi'an 710072, China; [2]Key Laboratory of Optoelectronic Technology and Systems (Ministry of Education), Chongqing University, Chongqing 400044, China; [3]MOE Key Laboratory of Weak-Light Nonlinear Photonics, TEDA Applied Physics Institute and School of Physics, Nankai University, Tianjin 300457, China

* Correspondence: W D Zhang, Email: zhangwd@nwpu.edu.cn; T Mei, Email: ting.mei@ieee.org

This file includes:

Supplementary information is available for this paper at https://doi.org/10.29026/oea.2018.180010

Section 1: Derivation of eigenvalue equation

A silver cylinder, with cylindrical interface infinitely extending along the z axis, is surrounded with air. $\varepsilon_{\mathrm{Ag}}$ and ε_{d} are the dielectric permittivity of the silver and air, respectively. The amplitudes E_z, H_z, E_ρ, H_ρ, E_φ, H_φ are the components of the cylindrical electromagnetic field propagation along the z axis which are defined by harmonics of the form: $U_{jm}(\rho)\exp(\pm \mathrm{i}m\varphi \pm \mathrm{i}qz)$, j=1, 2; m=0, 1, 2, 3, where U_{jm} are cylindrical functions of order m and the radial coordinate ρ. These amplitudes are shown in Table 1, in which R is radius of the sliver cylinder.

Table 1 | Cylindrical interface own mode components[1]

U_j	Core: $\rho \le R, j=1$	Cladding: $\rho \ge R, j=2$
E_z	$A_1 I_m(\chi_1\rho)$	$A_2 K_m(\chi_2\rho)$
H_z	$B_1 I_m(\chi_1\rho)$	$B_2 K_m(\chi_2\rho)$
E_ρ	$A_1 I'_m(\chi_1\rho)\frac{q}{i\chi_1} - B_1 I_m(\chi_1\rho)\frac{mk_0}{\chi_1^2\rho}$	$A_2 K'_m(\chi_2\rho)\frac{q}{i\chi_2} - B_2 K_m(\chi_2\rho)\frac{mk_0}{\chi_2^2\rho}$
H_ρ	$B_1 I'_m(\chi_1\rho)\frac{q}{i\chi_1} + A_1 I_m(\chi_1\rho)\frac{\varepsilon_{Ag}mk_0}{\chi_1^2\rho}$	$B_2 K'_m(\chi_2\rho)\frac{q}{i\chi_2} + A_2 K_m(\chi_2\rho)\frac{\varepsilon_d mk_0}{\chi_2^2\rho}$
E_φ	$B_1 I'_m(\chi_1\rho)\frac{k_0}{i\chi_1} + A_1 I_m(\chi_1\rho)\frac{mq}{\chi_1^2\rho}$	$B_2 K'_m(\chi_2\rho)\frac{k_0}{i\chi_2} + A_2 K_m(\chi_2\rho)\frac{mq}{\chi_2^2\rho}$
H_φ	$-A_1 I'_m(\chi_1\rho)\frac{k_0\varepsilon_{\mathrm{Ag}}}{i\chi_1} + B_1 I_m(\chi_1\rho)\frac{mq}{\chi_1^2\rho}$	$-A_2 K'_m(\chi_2\rho)\frac{k_0\varepsilon_{\mathrm{d}}}{i\chi_2} + B_2 K_m(\chi_2\rho)\frac{mq}{\chi_2^2\rho}$
	$\chi_1^2 = \beta^2 - k_0^2\varepsilon_{\mathrm{Ag}}$	$\chi_2^2 = \beta^2 - k_0^2\varepsilon_{\mathrm{d}}$

I_m — modified Bessel function of order m; $I'_m(x) = \mathrm{d}I_m / \mathrm{d}x$.
K_m — modified Hankel function of order m; $K'_m(x) = \mathrm{d}K_m / \mathrm{d}x$.

Based on the electromagnetic field components in Table 1 and the corresponding boundary conditions of electromagnetic field components, the relationship between A_1 and A_2, B_1 and B_2 can be written as

$$\begin{cases} A_2 = A_1 \dfrac{I_m(\chi_1\rho)}{K_m(\chi_2\rho)} \\ B_2 = B_1 \dfrac{I_m(\chi_1\rho)}{K_m(\chi_2\rho)} \end{cases}, \tag{1}$$

$$\begin{cases} B_1 I'_m(\chi_1\rho)\dfrac{k_0}{i\chi_1} + A_1 I_m(\chi_1\rho)\dfrac{mq}{\chi_1^2\rho} = B_2 K'_m(\chi_2\rho)\dfrac{k_0}{i\chi_2} + A_2 K_m(\chi_2\rho)\dfrac{mq}{\chi_2^2\rho} \\ -A_1 I'_m(\chi_1\rho)\dfrac{k_0\varepsilon_{Ag}}{i\chi_1} + B_1 I_m(\chi_1\rho)\dfrac{mq}{\chi_1^2\rho} = -A_2 K'_m(\chi_2\rho)\dfrac{k_0\varepsilon_d}{i\chi_2} + B_2 K_m(\chi_2\rho)\dfrac{mq}{\chi_2^2\rho} \end{cases}. \tag{2}$$

Substituting Eq. (1) into Eq. (2), a system of homogeneous equations for A_1 and B_1 can be expressed as

$$\begin{cases} I_m(\chi_1\rho)\left(\dfrac{mq}{\chi_1^2\rho} - \dfrac{mq}{\chi_2^2\rho}\right)A_1 + \left[I'_m(\chi_1\rho)\dfrac{k_0}{i\chi_1} - \dfrac{I_m(\chi_1\rho)}{K_m(\chi_2\rho)}K'_m(\chi_2\rho)\dfrac{k_0}{i\chi_1}\right]B_1 = 0 \\ \left[-I'_m(\chi_1\rho)\dfrac{k_0\varepsilon_{Ag}}{i\chi_1} + \dfrac{I_m(\chi_1\rho)}{K_m(\chi_2\rho)}K'_m(\chi_2\rho)\dfrac{k_0\varepsilon_d}{i\chi_1}\right]A_1 + I_m(\chi_1\rho)\left(\dfrac{mq}{\chi_1^2\rho} - \dfrac{mq}{\chi_2^2\rho}\right)B_1 = 0 \end{cases}. \tag{3}$$

Eq. (3) can be further written as

$$\begin{bmatrix} M_1 & N_1 \\ M_2 & N_2 \end{bmatrix}\begin{bmatrix} A_1 \\ B_1 \end{bmatrix} = 0 \quad . \tag{4}$$

where

$$\begin{cases} M_1 = I_m(\chi_1\rho)\left(\dfrac{mq}{\chi_1^2\rho}-\dfrac{mq}{\chi_2^2\rho}\right) \\ N_1 = I'_m(\chi_1\rho)\dfrac{k_0}{i\chi_1}-\dfrac{I_m(\chi_1\rho)}{K_m(\chi_2\rho)}K'_m(\chi_2\rho)\dfrac{k_0}{i\chi_1} \\ M_2 = -I'_m(\chi_1\rho)\dfrac{k_0\varepsilon_{Ag}}{i\chi_1}+\dfrac{I_m(\chi_1\rho)}{K_m(\chi_2\rho)}K'_m(\chi_2\rho)\dfrac{k_0\varepsilon_d}{i\chi_1} \\ N_2 = I_m(\chi_1\rho)\left(\dfrac{mq}{\chi_1^2\rho}-\dfrac{mq}{\chi_2^2\rho}\right) \end{cases} \tag{5}$$

For TM_{01} mode, m=0 and H_z=0, thus B_1=B_2=0. So that M_1=M_2=0 in Eq. (5). If there is a solution to TM_{01} mode, A_1 and B_1 in Eq. (4) cannot be all equal to zero, thus the characteristic determinant of Eq. (4) must equal to zero, and can be expressed as

$$-I'_0(\chi_1\rho)\frac{k_0\varepsilon_{Ag}}{i\chi_1}+\frac{I_0(\chi_1\rho)}{K_0(\chi_2\rho)}K'_0(\chi_2\rho)\frac{k_0\varepsilon_d}{i\chi_1}=0 \quad . \tag{6}$$

In addition, taking account of $I'_0=I_1$, $K'_0=-K_1$, Eq. (6) can be written as

$$\frac{I_1(\chi_1 R)}{I_0(\chi_1 R)}\frac{\varepsilon_{Ag}}{\chi_1}=-\frac{K_1(\chi_2 R)}{K_0(\chi_2 R)}\frac{\varepsilon_d}{\chi_2} \quad . \tag{7}$$

That is the eigenvalue equation of TM_{01} mode.

Similarly, for HE_{mn}/EH_{mn} mode, $m\neq0$; $H_z\neq0$ and $E_z\neq0$, thus $B_1\neq0$, $A_1\neq0$. The characteristic determinant of Eq. (4) must be equal to zero, and can be expressed as

$$\left(\frac{mq}{\chi_1^2\rho}-\frac{mq}{\chi_2^2\rho}\right)^2=\left[\frac{I'_m(\chi_1\rho)}{I_m(\chi_1\rho)}\frac{k_0}{\chi_1}-\frac{K'_m(\chi_2\rho)}{K_m(\chi_2\rho)}\frac{k_0}{\chi_2}\right]\left[\frac{I'_m(\chi_1\rho)}{I_m(\chi_1\rho)}\frac{k_0\varepsilon_{Ag}}{\chi_1}-\frac{K'_m(\chi_2\rho)}{K_m(\chi_2\rho)}\frac{k_0\varepsilon_d}{\chi_2}\right]. \tag{8}$$

Let $W_1=\chi_1\rho$, $W_2=\chi_2\rho$, Eq. (8) can be obatined as

$$m^2\left(\frac{1}{W_1^2}-\frac{1}{W_2^2}\right)\left(\frac{\varepsilon_{Ag}}{W_1^2}-\frac{\varepsilon_d}{W_2^2}\right)=\left[\frac{1}{W_1}\frac{I'_m(W_1)}{I_m(W_1)}-\frac{K'_m(W_2)}{K_m(W_2)}\frac{1}{W_2}\right]\left[\frac{I'_m(W_1)}{I_m(W_1)}\frac{\varepsilon_{Ag}}{W_1}-\frac{K'_m(W_2)}{K_m(W_2)}\frac{\varepsilon_d}{W_2}\right]. \tag{9}$$

Eq. (9) can be simplified as

$$m^2\left(\frac{1}{W_1^2}-\frac{1}{W_2^2}\right)\left(\frac{\varepsilon_{Ag}}{W_1^2}-\frac{\varepsilon_d}{W_2^2}\right)=(S-T)\left(\varepsilon_{Ag}S-\varepsilon_d T\right) \quad , \tag{10}$$

where

$$S=\frac{1}{W_1}\frac{I'_m(W_1)}{I_m(W_1)} \quad , \quad T=\frac{1}{W_2}\frac{K'_m(W_2)}{K_m(W_2)} \quad . \tag{11}$$

Furthermore, Eq. (10) can be written as

$$S=\frac{T}{2}\left(1+\frac{\varepsilon_d}{\varepsilon_{Ag}}\right)\pm\frac{1}{2}\sqrt{\left(1+\frac{\varepsilon_d}{\varepsilon_{Ag}}\right)^2T^2-4\left[\frac{\varepsilon_d}{\varepsilon_{Ag}}T^2-m^2\left(\frac{1}{W_1^2}-\frac{1}{W_2^2}\right)\left(\frac{1}{W_1^2}-\frac{\varepsilon_d}{\varepsilon_{Ag}}\frac{1}{W_2^2}\right)\right]} \quad , \tag{12}$$

where '±' represents the eigenvalue equation of EH_{mn} and HE_{mn} modes, respectively. Additionally, since the radial number of EH_{mn}/HE_{mn} mode can only take n=1, as the radial field distribution has only one maximum at the metal-air interface. And for each order m, there is only one solution for Eq. (12), that is HE_{m1} mode for $m\geq1$[2].

Section 2: Enhancement factor of the silver tip directly illuminated by far-filed excitation light

We compared the enhancement factor (EF) of the grating-assisted coupling silver tip with far-filed excitation light directly illuminating the silver tip (Fig. S1(a)). The excitation field TFSF with polarization parallel to the tip axis is used in this case. Figures S1(b) and S1(d) show the non-gap and gap mode electric field intensity distributions located 1 nm below the tip apex, respectively. Due to the propagating loss, the EF of grating-assisted tip is smaller than that of direction illumination of the silver tip with far-filed excitation light. However, the EF of grating-assistant tip is still within an acceptable range[3].

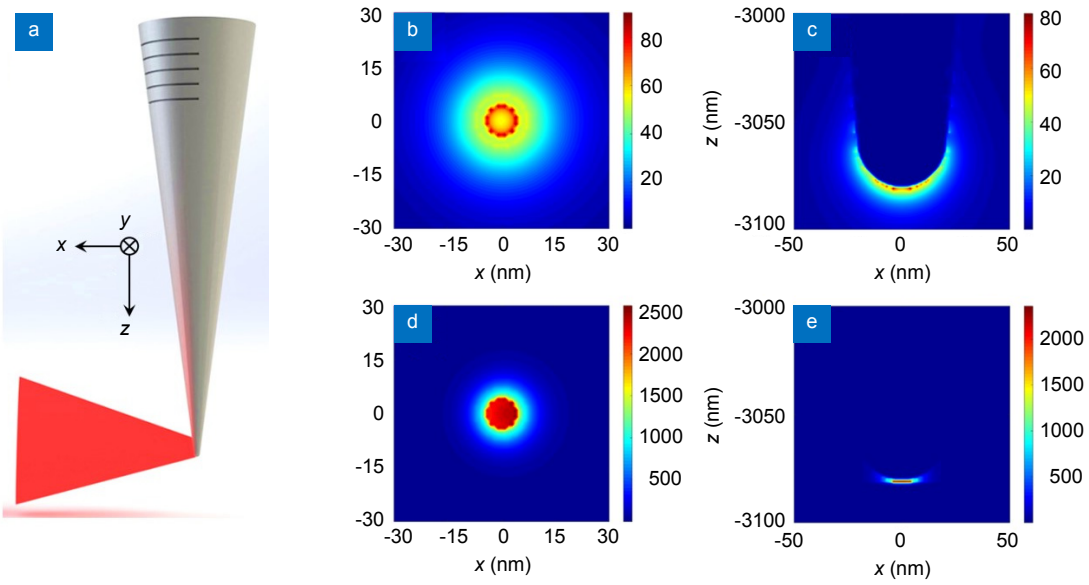

Fig. S1 | (**a**) Sketch map of the silver tip directly illuminated by far-filed excitation light; Non-gap (**b**) and gap mode (**d**) electric field intensity distribution located 1 nm below the silver tip; Non-gap (**c**) and gap mode (**e**) electric intensity distribution in the *x*-*z* plane.

Supplementary information references

1. Gurevich V S, Libenson M N. Surface-Polaritons Propagation Along Micropipettes. *Ultramicroscopy* **57**, 277–281 (1995).
2. Novotny L, Hafner C. Light propagation in a cylindrical waveguide with a complex, metallic, dielectric function. *Phys Rev E* **50**, 4094–4106 (1994).
3. Kazemi-Zanjani N, Vedraine S, Lagugné-Labarthet F. Localized enhancement of electric field in tip-enhanced Raman spectroscopy using radially and linearly polarized light. *Opt Express* **21**, 25271 (2013).